Published in final edited form as:
Diabetes. 2007 May ; 56(5): 1341–1349. doi:10.2337/db06-1619.

Pharmacological Inhibition of Glucosylceramide Synthase Enhances Insulin Sensitivity

Johannes M. Aerts[1], **Roelof Ottenhoff**[2], **Andrew S. Powlson**[3], **Aldo Grefhorst**[4], **Marco van Eijk**[2], **Peter F. Dubbelhuis**[2], **Jan Aten**[4], **Folkert Kuipers**[5], **Mireille J. Serlie**[6], **Tom Wennekes**[7], **Jaswinder K. Sethi**[3], **Stephen O'Rahilly**[3], and **Hermen S. Overkleeft**[7]

[1]Department of Medical Biochemistry, Academic Medical Center, University of Amsterdam, Amsterdam, the Netherlands [2]Macrozyme, Amsterdam, the Netherlands [3]Department of Clinical Biochemistry, University of Cambridge, Cambridge, U.K. [4]Department of Pathology, Academic Medical Center, University of Amsterdam, Amsterdam, the Netherlands [5]Centre for Liver, Digestive, and Metabolic Disease, Academic Hospital Groningen, University of Groningen, Groningen, the Netherlands [6]Department of Endocrinology and Metabolism, Academic Medical Center, University of Amsterdam, Amsterdam, the Netherlands [7]Gorlaeus Laboratories, Leiden Institute of Chemistry, Leiden University, Leiden, the Netherlands

Abstract

A growing body of evidence implicates ceramide and/or its glycosphingolipid metabolites in the pathogenesis of insulin resistance. We have developed a highly specific small molecule inhibitor of glucosylceramide synthase, an enzyme that catalyzes a necessary step in the conversion of ceramide to glycosphingolipids. In cultured 3T3-L1 adipocytes, the iminosugar derivative *N*-(5′-adamantane-1′-yl-methoxy)-pentyl-1-deoxynojirimycin (AMP-DNM) counteracted tumor necrosis factor-α-induced abnormalities in glycosphingo-lipid concentrations and concomitantly reversed abnormalities in insulin signal transduction. When administered to mice and rats, AMP-DNM significantly reduced glycosphin-golipid but not ceramide concentrations in various tissues. Treatment of *ob/ob* mice with AMP-DNM normalized their elevated tissue glucosylceramide levels, markedly lowered circulating glucose levels, improved oral glucose tolerance, reduced A1C, and improved insulin sensitivity in muscle and liver. Similarly beneficial metabolic effects were seen in high fat-fed mice and ZDF rats. These findings provide further evidence that glycosphingolipid metabolites of ceramide may be involved in mediating the link between obesity and insulin resistance and that interference with glycosphingolipid biosynthesis might present a novel approach to the therapy of states of impaired insulin action such as type 2 diabetes.

Obesity is strongly associated with insulin resistance, but the underlying pathogenic mechanism is still an enigma. The strong correlation between insulin resistance and intramyocellular lipid levels suggests that excessive exposure to lipids or their metabolites,

Address correspondence and reprint requests to J.M. Aerts, Department of Medical Biochemistry, Academic Medical Center, University of Amsterdam, Meibergdreef 15, 1105AZ, Amsterdam, Netherlands. j.m.aerts@amc.uva.nl.

Additional information for this article can be found in an online appendix at http://dx.doi.org/10.2337/db06-1619.

Europe PMC Funders Author Manuscripts

so-called lipotoxicity, may play a crucial role (1-5). The rapid induction of insulin resistance in rodents by infusions with palmitate has directed attention to the sphingolipid ceramide as a potential mediator of insulin resistance (1,4,5). Palmitate is a critical precursor in the synthesis of ceramide, and its enhanced supply inevitably increases sphingolipid formation in tissues (5,6). Increased ceramide concentrations (twofold) have indeed been observed in skeletal muscle from obese insulin-resistant individuals (4). The pivotal role of ceramide in insulin resistance and lipotoxicity has been recently extensively reviewed (5). It is of interest to note that ceramide is also considered a molecular link between inflammation and insulin resistance (7).

Obesity triggers a chronic inflammatory state, and cytokines like tumor necrosis factor (TNF)-α released from either adipocytes or from macrophages infiltrating adipose tissue antagonize insulin action. The well-established induction of insulin resistance by TNF-α is thought to be attributable to its ability to promote sphingolipid biosynthesis, as has been demonstrated at both mRNA and cellular lipid levels (5,7-10). Several investigations with cultured cells have linked excessive ceramide concentrations to disturbed insulin signaling (5). Manipulation of ceramide concentrations in cultured cells was consistently found to affect the insulin signaling pathway downstream of Akt, but conflicting reports exist regarding effects on the insulin receptor, IRS-1, and associated phosphatidylinositol 3-kinase activity (5,9-11). More recently, potentially important roles for protein kinase-Cζ, Jun NH_2-terminal kinase, and IκKβ (Iκ-B kinase-β) in the regulation of insulin signaling have been recognized. Ceramide has been shown to initiate signaling pathways leading to the activation of both Jun NH_2-terminal kinase and IκKβ (5,11,12), processes that would support an insulin-resistant phenotype. Although there are compelling literature reports pointing to direct and indirect antagonistic effects of ceramide on the insulin signaling pathway, an additional role for glycosphingolipid metabolites of ceramide in the development of insulin resistance also has to be considered. Glycosphingolipids are found in specific (detergent-resistant) membrane microdomains in close physical proximity to the insulin receptor, as well as other tyrosine kinase receptors such as the epidermal growth factor receptor (13). A regulatory role for glycosphingolipids in hormone sensitivity was first proposed by Bremer and colleagues (14) who showed that epidermal growth factor–mediated signaling is inhibited by the ganglioside sialosyllactosylceramide (GM3). More recently, Tagami et al. (15) reported that addition of GM3 to cultured adipocytes also suppresses phosphorylation of the insulin receptor and its downstream substrate IRS-1, resulting in reduced glucose uptake. Other observations further substantiate the role of the ganglioside GM3 in responsiveness to insulin. Mutant mice lacking GM3 show an enhanced phosphorylation of the skeletal muscle insulin receptor after ligand binding and are protected from high-fat diet–induced insulin resistance (16). Conversely, GM3 levels are elevated in the muscle of certain obese, insulin-resistant mouse and rat models (15). Inokuchi and colleagues (15) used the ceramide analog 1-phenyl-2-decanoylamino-3-morpholinopropanol (PDMP), an inhibitor of glucosylceramide synthase, to reduce glycosphingolipids in cultured adipocytes. They noted that PDMP counteracted the inhibitory effects of TNF-α on insulin receptor and IRS-1 phosphorylation. More recently, it was reported by the same researchers that high GM3 levels diminished insulin receptor accumulation in detergent-resistant membrane microdomains and insulin-dependent IR

internalization (17). Again, glycosphingolipid depletion by incubation of cells with PDMP prevented these abnormalities. However, the observations made with PDMP are difficult to interpret since this compound also inhibits transacylation to 1-*O*-acylceramide and consequently increases cellular concentrations of ceramide (18).

Based on the present information, it may be conceived that not just ceramide itself but rather its glycosphingo-lipid metabolites are instrumental in the development of insulin resistance. To discriminate between these possibilities, we examined in obese rodents the effect of reduction of glycosphingolipids by *N*-(5′-adamantane-1′-yl-methoxy)-pentyl-1-deoxynojirimycin (AMP-DNM), a specific inhibitor of glucosylceramide synthase (19). Here we show that pharmacological lowering of glycosphingolipids, without significant reduction of ceramide, dramatically reverses insulin resistance in in vitro and in vivo models.

RESEARCH DESIGN AND METHODS

Experimental procedures were all approved by the appropriate ethics committee for animal experiments. C57Bl/6J and *ob/ob* mice (C57Bl/6J background) were obtained from Harlan (Horst, the Netherlands) and ZDF (ZDF/GMi-*fa/fa*) rats from Charles River Laboratories (Wilmington, MA). Animals were fed a commercially available lab diet (RMH-B; Hope Farms, Woerden, the Netherlands). To induce glucose intolerance in C57Bl/6J mice, animals were fed a high-fat diet (16.4% protein, 25.5% carbohydrates, and 58.0% fat) for 4 weeks. The iminosugar AMP-DNM was mixed in the food or, when indicated, administered by oral gavage two times daily.

Plasma and tissue sampling

Blood samples were collected by either tail vein or retroorbital plexus puncture. A large blood sample was collected by cardiac puncture. Tissues were quickly removed and frozen for further analysis.

Cells

3T3-L1 preadipocytes were obtained from American *Type Culture* Collection (Manassas, VA). They were propagated and differentiated as previously described (20).

Iminosugar

AMP-DNM was synthesized as described (21). Plasma levels of AMP-DNM were determined by mass spectrometry, following high-pressure liquid chromatography (Xendo, Groningen, the Netherlands).

Analysis of lipids and measurement of enzyme activities

Lipids were extracted according to Folch et al. (22). Ceramide and glucosylceramide were determined by high-performance liquid chromatography (HPLC) analysis of orthophtaldehyde-conjugated lipids according to a procedure previously described with some modifications (23). Deacylation of lipids was performed in 0.5 ml 0.1 mol/l NaOH in methanol in a microwave oven (CEM microwave Solids/Moisture System SAM-155).

Deacylated glycolipids were derivatized on line for 30 min with *O*-phtaldehyde. Analysis was performed using an HPLC system (Waters Associates, Milford, MA) and a Hypersil BDS C18 3μ, 150 × 4.6–mm reverse-phase column (Alltech). Ganglioside composition was determined by analysis of the acidic glycolipid fraction obtained after Folch extraction. Gangliosides were quantified by densitometry after high-performance thin-layer chromatography separation, spraying with resorcinol reagent, and heating at 105°C for 10 min. Alternatively, gangliosides were quantified following HPLC separation of oligosaccharides released from glycolipids by ceramide glycanase digestion (24). Activity of glucosylceramide synthase and glucocerebrosidase in living cells was determined using, as substrates, fluorescently labeled NBD (4-fluoro-7-nitrobenz-2-oxa-1,3-diazole)-ceramide and -glucosylceramide, respectively (25). Half-maximal inhibitory concentration (IC_{50}) values of AMP-DNM for various enzymes were determined by exposing cells or enzyme preparations to an appropriate range of iminosugar concentrations. Lactase, maltase, and sucrase were determined with homogenates of freshly isolated rat intestine using assay conditions described earlier (26). Debranching enzyme (α-1, 6-glucosidase) was measured with an erythrocyte preparation as enzyme source (27).

Analysis of insulin signaling in cultured human and 3T3-L1 adipocytes

Fully differentiated 3T3-L1 adipocytes were serum deprived, by incubation in Dulbecco's modified Eagle's medium plus 1% BSA, and simultaneously pre-treated with or without AMP-DNM (10 μmol/l) and/or TNF-α (0.6 nmol/l) for 24 h. Following insulin stimulation (5 min with 100 nmol/l), cells were washed with ice-cold PBS and lysed in modified radioimmunoprecipitation assay buffer (28). Cell lysates were clarified by centrifugation (13,000 rpm for 10 min). Equal amounts of whole-cell lysates were separated by SDS-PAGE and immunoblots performed in parallel using antiphosphotyrosine antibody (4G10), anti–IRS-1 (Upstate), anti-IR (K. Siddle, Department of Clinical Biochemistry, University of Cambridge, Cambridge, U.K.), anti-pSer473 Akt (Cell Signaling Technology), appropriate horseradish peroxidase (HRP)-linked secondary antibody (Dako), and an enzyme-linked chemiluminescent kit (Amersham) (28).

Analysis of insulin signaling in liver

Mice were fasted for 4 h, and insulin (0.75 units/kg body wt) was administered intravenously. After 5 min, animals were killed and livers were collected and lysed in modified radioimmunoprecipitation assay buffer as described above. Equal amounts of lysates were separated by SDS-PAGE, and immunoblots were performed using appropriate antibodies (Santa Cruz Biotechnology).

Measurement of whole-body insulin sensitivity

Whole-body insulin sensitivity of *ob/ob* mice was determined using hyperinsulinemic-euglycemic clamps as previously described (29,30). Male *ob/ob* mice were treated for 7 days with a diet with or without AMP-DNM (25 mg/kg body wt). All values represent mean ± SE for the number of animals indicated. Analyses were performed using SPSS for Windows software (SPSS, Chicago, IL).

Analysis of pancreatic tissue

For insulin and glucagon staining, sections were incubated with either HRP-conjugated guinea pig IgG anti-rat insulin (Crystal Chem, Downers Grove, IL) or a rabbit antihuman glucagon (Dako-Cytomation, Glostrup, Denmark) and appropriate HRP-linked secondary antibody. Glucose tolerance tests were performed in fasted animals (>6 h) with oral gavage of glucose (1 or 2 g glucose/kg body wt). Blood glucose values were measured immediately before and 120 min after glucose injection. Area under the curve (AUC) (arbitrary units per minute) were determined for individual animals.

Cell surface expression of GM3

Flow cytometry using monoclonal anti-GM3 antibody (Seikagu) and fluorescein isothiocyanate– or Alexa 488–conjugated secondary antibodies were used according to the procedure described earlier (15).

Statistical testing

Values presented in figures represent means ± SE. Statistical analysis of two groups was assessed by Student's *t* test (two tailed) or ANOVA for repeated measurement (clamp experiment). Level of significance was set at $P < 0.05$.

RESULTS

Modulation of glycosphingolipids with AMP-DNM

Hydrophobic *N*-alkylated deoxynojirimycins, in particular AMP-DNM, are potent inhibitors of glucosylceramide synthase (19,31). Exposure of cells to AMP-DNM results in swift inhibition of synthesis of glucosylceramide. The apparent IC_{50} values range from 150 to 220 nmol/l in various cell types. Cellular concentrations of glucosylceramide and gangliosides are gradually reduced by AMP-DNM, reaching equilibrium within 36 h. Ceramide levels, however, remain constant on exposure to AMP-DNM. Drug treatment does not change mRNA encoding glucosyl-ceramide synthase (not shown). No changes in cellular levels of diacylglycerol, sphingomyelin, or phosphatidylcholine are observed following prolonged AMP-DNM treatment of cells. At high concentrations (>1 μmol/l), AMP-DNM also significantly inhibits lysosomal glucocere-brosidase activity (19).

Effect of AMP-DNM on glycosphingolipid levels and insulin sensitivity of cultured 3T3-L1 adipocytes

To study the effect of AMP-DNM in a robust cellular model of insulin resistance, cultured 3T3-L1 adipocytes were incubated with TNF-α. As expected, TNF-α impaired insulin receptor autophosphorylation, IRS-1 tyrosine phosphorylation, and Ser-473 phosphorylation of Akt. All of these abnormalities were significantly ameliorated by the simultaneous exposure of cells to 10 μmol/l AMP-DNM (Fig. 1, *upper panel*). TNF-α increased cell surface levels of GM3 gangliosides, and this was blocked by AMP-DNM (Fig. 1, *lower panel*). Quantification by HPLC revealed that ceramide and gangliosides were elevated by TNF-α. The increase of the gangliosides GM3 and GM2 induced by the cytokine, but not that of ceramide, was counteracted by the iminosugar AMP-DNM (Table 1).

Europe PMC Funders Author Manuscripts

Reduction of glycosphingolipids in normal mice and rats by AMP-DNM

AMP-DNM is well tolerated by rodents when administered by gavage or mixed in the food. AMP-DNM does not accumulate with daily exposure over 28 days. No significant in vivo metabolism of the compound could be demonstrated by mass spectrometric analysis of urine and plasma samples. More than 90% of AMP-DNM was recovered after in vitro incubation with microsomes for 4 h (not shown). Iminosugar administration to rodents up to concentrations of 100 mg · kg^{-1} · day^{-1} for 2 months did not result in any overt toxicity. The plasma half-life of AMP-DNM was ~3.1 and 4.2 h in mice and rats, respectively. After oral administration of 25 mg AMP-DNM/kg body wt, maximal plasma concentrations of 5 μmol/l AMP-DNM were reached at 30 min.

To study the effect on tissue glycosphingolipid levels, 6-week-old C57Bl/6J mice (n = 4) were treated with or without AMP-DNM at a dose of 25 mg · kg body wt^{-1} · day^{-1} for 14 days. The mean ± SE plasma concentration of AMP-DNM, 108 ± 6 nmol/l, remained stable during the period of treatment. After treatment, ceramide and glucosylceramide concentrations in liver and muscle were determined (Table 2). The hepatic ceramide content of C57Bl/6J mice was not changed by the AMP-DNM diet. In sharp contrast, liver glucosylceramide was reduced by 41 ± 5%. Quantification of the ganglioside GM3 by HPLC revealed that the lipid was reduced by 28 ± 6% in liver of AMP-DNM-treated mice. Similar effects on sphingolipids were observed in muscle tissue (Table 2). Unfortunately, accurate determination of glycosphingolipid concentrations in adipose tissue proved technically not feasible due to marked interference of the large amounts of triglycerides in the analytic procedures, causing very high intra-assay coefficients of variation (>35%).

Ceramide and glycosphingolipids in *ob/ob* mice before and after treatment with AMP-DNM

Leptin-deficient *ob/ob* mice spontaneously develop obesity and associated insulin resistance. Analysis of glycosphingolipids revealed that the hepatic concentration of glucosylceramide was higher in *ob/ob* mice (115 ± 16 nmol/liver) compared with matched wild-type animals (85 ± 15 nmol/liver; P = 0.045) (Table 2). In muscle tissue of *ob/ob* mice, glucosylceramide was again elevated compared with wild-type mice (P = 0.031); however, ceramide concentrations were similar (Table 2). Two weeks' treatment of *ob/ob* mice with 25 mg AMP-DNM · kg^{-1} · day^{-1} did not result in any significant changes in ceramide concentrations in muscle or liver. In sharp contrast, glucosylceramide content of muscle and liver from *ob/ob* mice decreased by 45 ± 23 and 45 ± 11%, respectively, with AMP-DNM, reaching values similar to those in wild-type animals (Table 2).

Beneficial effects of AMP-DNM on metabolism in *ob/ob* mice

To investigate whether signaling is improved by AMP-DNM, mice were killed 5 min after insulin administration. Figure 2 shows that insulin signaling in the liver is improved by AMP-DNM in a dose-dependent manner, as indicated by increased phosphorylation of the insulin receptor and mTOR.

Prominent effects of AMP-DNM on glucose homeostasis were noted when *ob/ob* mice (n = 4) were treated at a dose of 25 mg · kg body wt^{-1} · day^{-1}. AMP-DNM had no significant effect on body weight or food intake (Fig. 3*A*) but concomitantly led to a pronounced

reduction in blood glucose concentrations ($P = 0.008$) (Fig. 3*B*). Hyperinsulinemic-euglycemic clamp studies demonstrated that this was associated with a marked improvement in whole-body insulin sensitivity ($P = 0.003$) (Fig. 3*C*). This was due in part to a significant (~26%) decrease in hepatic glucose production (R_a) ($P = 0.035$) as well as a significant (~29%) increase in glucose disposal (R_d) ($P = 0.0028$) (Fig. 3*D*).

The beneficial effect of AMP-DNM was also revealed by glucose tolerance tests. Animals fed with 25 mg/kg AMP-DNM for 8 days showed a better response to oral glucose administration (1 g/kg body wt) compared with untreated mice. The AUCs of blood glucose concentrations were significantly lower ($P = 0.023$) in AMP-DNM-treated mice (13.21 ± 1.43 [SD] compared with 20.15 ± 2.33). A marked reduction was also observed in A1C in *ob/ob* mice receiving 25 mg AMP-DNM · kg body wt^{-1} · day^{-1} for 9 weeks. The A1C concentration was 4.82 ± 0.85% in the treated *ob/ob* mice compared with 6.82 ± 0.88% in the untreated animals and 4.31 ± 0.66% in corresponding wild-type mice. Hepatic fat accumulation was apparent in untreated *ob/ob* mice, and this was reduced by AMP-DNM therapy. Triglyceride concentrations in livers of AMP-DNM–fed *ob/ob* mice were significantly decreased from 107 ± 13 to 80 ± 11 nmol/mg liver ($P = 0.035$). Comparable treatment of normal C57Bl/6J mice with AMP-DNM did not result in reduction of blood glucose or A1C. No changes occurred in insulin concentration in fasted blood samples (not shown).

Effects of AMP-DNM in Zucker diabetic *fa/fa* rats

Male ZDF rats spontaneously develop pronounced obesity accompanied by marked insulin resistance and subsequent hypoinsulinemic diabetes. To test the efficacy of AMP-DNM in this model, we examined 8-week-old ZDF rats that were treated for 9 weeks with 0, 5, or 25 mg AMP-DNM · kg^{-1} · day^{-1} ($n = 4$ for each group). Body weights of ZDF rats receiving AMP-DNM were not significantly different from those of untreated animals.

Table 3 shows that treatment with a dose of 25 mg AMP-DNM · kg body wt^{-1} · day^{-1} resulted in a clear reduction in hepatic concentrations of glucosylceramide and gangliosides but did not change ceramide levels. Similar observations were made for muscle (not shown). Marked improvements in fasted and nonfasted blood glucose became already apparent within 1 week of treatment (Fig. 4*A* and *B*). Around 3 weeks of treatment, the ZDF rats receiving 25 mg AMP-DNM · kg^{-1} · day^{-1} showed close to normal fasted and nonfasted blood glucose concentrations, but, subsequently, blood glucose levels gradually rose. Before treatment, 8-week-old ZDF rats were already hyperinsulinemic (Fig. 4*C*). During the treatment period, insulin production in placebo-treated ZDF rats markedly diminished. In rats treated with 25 mg AMP-DNM · kg^{-1} · day^{-1}, hyperinsulinemia improved but was not completely corrected (Fig. 4*C*). Oral glucose tolerance tests conducted at weeks 2 and 9 of the treatment period revealed significantly improved glucose tolerance in ZDF rats receiving 25 mg AMP-DNM · kg^{-1} · day^{-1} ($P = 0.014$ and $P = 0.021$, respectively) (Fig. 4*D*). After 9 weeks of treatment, A1C in ZDF rats receiving the highest dose of AMP-DNM (6.31 ± 0.68%) was significantly reduced ($P = 0.0016$) compared with untreated ZDF rats (8.89 ± 0.33%) but still higher ($P = 0.012$) than in lean littermates (4.24 ± 0.1%) (Fig. 4*E*). Of note, there was a correlation between the ratio of hepatic glucosylceramide/ceramide in rats at the

end of the 9-week treatment period and A1C (Fig. 4*F*), providing support for the notion of a causal relationship between these two variables. We observed in a separate experiment that ZDF rats, treated for 10 weeks with a dose of 60 mg AMP-DNM · kg body wt^{-1} · day^{-1}, showed A1C levels (5.4 ± 0.4%) similar to normal littermates (5.3 ± 0.5%). AMP-DNM treatment of normal littermates of ZDF rats did not result in a reduction of blood glucose and A1C or cause changes in insulin concentrations in fasted blood samples (not shown).

The very low plasma insulin levels in 17-week-old placebo-treated ZDF rats indicate β-cell decomposition (Fig. 4*C*). The remaining high plasma insulin levels of drug-treated ZDF rats suggest some preservation of pancreatic β-cell function. Histological analysis of pancreatic tissue (Fig. 4*G-L*) revealed the presence of more insulin-producing β-cells in drug-treated ZDF rats (Fig. 4*J*) than in placebo controls (Fig. 4*H*) but clearly less than in lean littermates (Fig. 4*L*).

A consistent picture emerged from analysis of the insulin signaling pathway in livers collected from animals fasted for 6 h. Only the livers of the fasted ZDF rats receiving 25 mg AMP-DNM · kg^{-1} · day^{-1} showed marked insulin receptor autophosphorylation and serine phosphorylation of Akt, mTOR, and p70S6K (online appendix data [available at http://dx.doi.org/10.2337/db06-1619]). This finding is not surprising, since only these animals showed high insulin levels while fasted.

Effects of AMP-DNM in a murine model of diet-induced obesity and glucose intolerance

To induce glucose intolerance, C57Bl/6J mice were fed a high-fat diet for 4 weeks. Animals (n = 8 for each group) were treated by daily oral gavage for 2 weeks with different doses of AMP-DNM (0, 5, and 25 mg · kg^{-1} · day^{-1}). There were no significant differences in body weight between the different treatment groups (Fig. 5*A*). In the animals treated with 25 mg · kg^{-1} · day^{-1} AMP-DNM, fasting blood glucose (7.74 ± 0.40 [SD] mmol/l) was significantly lower than in animals treated with 0 or 5 mg · kg^{-1} · day^{-1} AMP-DNM (9.57 ± 0.38 and 9.46 ± 0.26 mmol/l, respectively) (Fig. 5*B*). After oral glucose load (1 g/kg body wt), the glycemic profile was significantly (P = 0.021) better in mice treated with the highest dose of AMP-DNM than in the other animals (AUC 9.72 ± 0.21, 12.24 ± 0.20, and 12.25 ± 0.29 for mice, 5 and 0 mg AMP-DNM · kg^{-1} · day^{-1}, respectively) (Fig. 5*C*). Plasma insulin concentrations tended to be lower in animals treated with 25 mg AMP-DNM · kg^{-1} · day^{-1} compared with the other two groups (Fig. 5*D*).

DISCUSSION

In these studies, we have demonstrated that AMP-DNM, a potent inhibitor of glucosylceramide synthase, has dramatic beneficial effects on the insulin resistance and hyperglycemia seen in ZDF rats, *ob/ob* mice, and high-fat diet–induced glucose-intolerant mice via a mechanism that does not require a reduction in food intake or loss of body weight. Interestingly, 17-week-old ZDF rats treated with 25 mg AMP-DNM · kg^{-1} · day^{-1} were still able to produce significant amounts of insulin in contrast to placebo-treated animals. Apparently, in this rodent diabetes model, the iminosugar treatment exerts a protective effect on the pancreas. Since AMP-DNM does not change oral glucose tolerance,

blood glucose concentrations, or plasma insulin levels in lean animals, it seems unlikely that the drug stimulates insulin secretion directly.

Inhibition of glucosylceramide synthase by AMP-DNM causes no concomitant accumulation of ceramide, suggesting the existence of some feedback in ceramide metabolism. A key question that arises relates to the specificity of AMP-DNM as an inhibitor of glucosylceramide synthase. At a concentration <1 μmol/l, AMP-DNM causes no significant inhibition of activity of the lysosomal enzymes glucocerebrosidase, sphingomyelinase, acid α-glucosidase, or the endoplasmic reticulum–trimming α-glucosidases. The cytosolic debranching enzyme and glycogen synthase are also unaffected at such concentrations (data not shown). AMP-DNM was originally developed as an inhibitor of a nonlysosomal glucosylceramidase (24). This enzyme is inhibited by AMP-DNM in the picomolar range (IC_{50} ~1 nmol/l). Cultured adipocytes or *ob/ob* mice exposed to low nanomolar concentrations of AMP-DNM do not show improved responsiveness to insulin. Inhibition of the nonlysosomal glucosylceramidase by AMP-DNM seems not to be sufficient to increase insulin sensitivity. The molecular identity of the nonlysosomal glucosylceramidase as GBA2 (β-glucosidase 2) has been recently established (32,33). Analysis of GBA2 knockout mice revealed impaired spermatogenesis, but, otherwise, the phenotype of the animals is normal (32). Iminosugars can also significantly inhibit intestinal glycosidases, thus reducing the rate of digestion and absorption of oligo- and polysaccharides. This may additionally contribute to the beneficial effects of AMP-DNM. However, AMP-DNM is only a low-affinity inhibitor of sucrase and maltase, with IC_{50} values for these enzymes of 4.5 and 18 μmol/l, respectively. Therefore, it appears highly unlikely that the AMP-DNM dose used would impact intestinal glycosidases. Finally, it is unlikely that AMP-DNM had significant nonspecific toxic effects, as food intake remained unchanged in treated rodents and no abnormalities were noted on histological examination of liver, kidney, and brain. Only modest (30–50%) increases of liver glycogen were observed during the first week of feeding *ob/ob* mice with the AMP-DNM diet. Subsequently, glycogen levels remained stable in the normal range of C57Bl/6J animals, suggesting that there was no marked inhibition of debranching enzyme. Analysis of gene expression in livers of AMP-DNM–treated *ob/ob* mice (n = 3) rendered no indications for any cytotoxicity.

Our studies with AMP-DNM may help to clarify the relationship between obesity, ceramides, and insulin resistance. First, we confirmed previous observations that liver tissue from insulin-resistant *ob/ob* mice had elevated levels of ceramide, glucosylceramide, and gangliosides and demonstrated that muscle tissue from these animals had increased glucosylceramide but normal ceramide concentrations. We then demonstrated that AMP-DNM had dramatic beneficial effects on insulin sensitivity without any change in ceramide concentrations but with a marked reduction in tissue levels of glucosylceramide. These observations strongly suggest that it is unlikely that the elevation in ceramide itself solely mediates the insulin resistance seen in *ob/ob* mice but that downstream metabolites of ceramide are also likely to be critically involved. Our studies in cultured 3T3-L1 adipocytes revealed that AMP-DNM reversed the adverse effects of TNF-α on several steps in the insulin signal transduction pathway. This effect was demonstrable at a proximal step, i.e.,

insulin receptor autophosphorylation, of interest because of the previously reported localization of GM3 gangliosides in plasma membrane subdomains containing the insulin receptor and the effect of genetic depletion of GM3 on insulin receptor autophosphorylation.

One iminosugar, *N*-hydroxyethyldeoxynojirimycin (Miglitol), is already registered as an oral agent for treating diabetes (34). The ancient use of iminosugar-rich mulberry leaves in the Far East to control hyperglycemia stimulated the development of this drug (35,36). The presumed mode of action of Miglitol is inhibition of intestinal glycosidase activities, thereby buffering monosaccharide assimilation (34). We have established that Miglitol does not inhibit glucosylceramide synthase; however, we cannot exclude that some proportion of the well-absorbed compound is metabolized to some structure that is capable of inhibiting glucosylceramide synthase.

In summary, our investigations indicate that the beneficial effects of hydrophobic iminosugars like AMP-DNM on hyperglycemia are largely mediated by reduction of excessive glycosphingolipids in tissues. These findings support the notion that glycosphingolipids may play a critical role in the mediation of lipotoxic insulin resistance and should encourage the further evaluation of this class of imino-sugar-based compounds for the treatment of human insulin resistance and diabetes.

Supplementary Material

Refer to Web version on PubMed Central for supplementary material.

ACKNOWLEDGMENTS

We gratefully acknowledge the indispensable scientific input of Alfred Meijer, Albert Groen, Rolf Boot, Louis Boon, and Ans Groener, who should be considered as equally important members of the study group. We acknowledge the technical assistance by Edward van Wezel, Theo van Dijk, Sijmen Kuiper, Anneke Strijland, Yuri van Geertruy, Cindy van Roomen, Wilma Donker, Karen Ghauharali, Peter Simons, Jos Out, and Judith Weerts and the support of the Wellcome Trust (to S.O.R. and A.P.) and the Biotechnology and Biological Sciences Research Council, U.K. (to J.S.).

Glossary

AMP-DNM	*N*-(5′-adamantane-1′-yl-methoxy)-pentyl-1-deoxynojirimycin
AUC	area under the curve
GM3	sialosyllactosylceramide
HPLC	high-performance liquid chromatography
HRP	horseradish peroxidase
PDMP	1-phenyl-2-decanoylamino-3-morpholinopropanol
TNF	tumor necrosis factor

REFERENCES

1. Unger RH. Minireview: weapons of lean body mass destruction: the role of ectopic lipids in the metabolic syndrome. Endocrinology. 2003; 144:5159–5165. [PubMed: 12960011]

2. Savage DB, Petersen KF, Shulman GI. Mechanisms of insulin resistance in humans and possible links with inflammation. Hypertension. 2005; 45:828–833. [PubMed: 15824195]
3. Hegarty BD, Furler SM, Ye J, Cooney GJ, Kraegen EW. The role of intramuscular lipid in insulin resistance. Acta Physiol Scand. 2003; 178:373–383. [PubMed: 12864742]
4. Adams JM 2nd, Pratipanawatr T, Berria R, Wang E, DeFronzo RA, Sullards MC, Mandarino LJ. Ceramide content is increased in skeletal muscle from obese insulin-resistant humans. Diabetes. 2004; 53:25–31. [PubMed: 14693694]
5. Summers SA. Ceramides in insulin resistance and lipotoxicity. Prog Lipid Res. 2006; 45:42–72. [PubMed: 16445986]
6. Kolter T, Proia RL, Sandhoff K. Combinatorial ganglioside biosynthesis. J Biol Chem. 2002; 277:25859–25862. [PubMed: 12011101]
7. Wellen KE, Hotamisligil GS. Inflammation, stress, and diabetes. J Clin Invest. 2005; 115:1111–1119. [PubMed: 15864338]
8. Peraldi P, Spiegelman B. TNF-alpha and insulin resistance: summary and future prospects. Mol Cell Biochem. 1998; 182:169–175. [PubMed: 9609126]
9. Miura A, Miura A, Kajita K, Ishizawa M, Kanoh Y, Kawai Y, Natsume Y, Sakuma H, Yamamoto Y, Yasuda K, Ishizuka T. Inhibitory effect of ceramide on insulin-induced protein kinase Czeta translocation in rat adipocytes. Metabolism. 2003; 52:19–24. [PubMed: 12524657]
10. Stratford S, Hoehn KL, Liu F, Summers SA. Regulation of insulin action by ceramide: dual mechanisms linking ceramide accumulation to the inhibition of Akt/protein kinase B. J Biol Chem. 2004; 279:26608–36615.
11. Powell DJ, Turban S, Gray A, Hajduch E, Hundal HS. Intracellular ceramide synthesis and PKCzeta activation play an essential role in palmitate-induced insulin resistance in rat L6 skeletal muscle cells. Biochem J. 2004; 382:619–629. [PubMed: 15193147]
12. Ruvolo PP. Intracellular signal transduction pathways activated by ceramide and its metabolites. Pharmacol Res. 2003; 47:383–392. [PubMed: 12676512]
13. Allende ML, Proia RL. Lubricating cell signalling pathways with gangliosides. Curr Opin Struct Biol. 2002; 12:587–592. [PubMed: 12464309]
14. Rebbaa A, Hurh J, Yamamoto H, Kersey DS, Bremer EG. Ganglioside GM3 inhibition of EGF receptor mediated signal transduction. Glycobiology. 1996; 6:399–406. [PubMed: 8842703]
15. Tagami S, Tagami S, Inokuchi Ji J, Kabayama K, Yoshimura H, Kitamura F, Uemura S, Ogawa C, Ishii A, Saito M, Ohtsuka Y, Sakaue S, Igarashi Y. Ganglioside GM3 participates in the pathological conditions of insulin resistance. J Biol Chem. 2002; 277:3085–3092. [PubMed: 11707432]
16. Yamashita T, Yamashita T, Hashiramoto A, Haluzik M, Mizukami H, Beck S, Norton A, Kono M, Tsuji S, Daniotti JL, Werth N, Sandhoff R, Sandhoff K, Proia RL. Enhanced insulin sensitivity in mice lacking ganglioside GM3. Proc Natl Acad Sci U S A. 2003; 100:3445–3449. [PubMed: 12629211]
17. Kabayama K, Kabayama K, Sato T, Kitamura F, Uemura S, Kang BW, Igarashi Y, Inokuchi J. TNF alpha-induced insulin resistance in adipocytes as a membrane microdomain disorder: involvement of ganglioside GM3. Glycobiology. 2004; 15:21–29. [PubMed: 15306563]
18. Shayman JA, Abe A, Hiraoka M. A turn in the road: how studies on the pharmacology of glucosylceramide synthase inhibitors led to the identification of a lysosomal phospholipase A2 with ceramide transacylase activity. Glycoconj J. 2004; 20:25–32. [PubMed: 14973367]
19. Aerts JM, Hollak C, Boot R, Groener A. Biochemistry of glycosphingolipid storage disorders: implications for therapeutic intervention. Philos Trans R Soc Lond B Biol Sci. 2003; 358:905–914. [PubMed: 12803924]
20. Nugent C, Prins JB, Whitehead JP, Savage D, Wentworth JM, Chatterjee VK, O'Rahilly S. Potentiation of glucose uptake in 3T3-L1 adipocytes by PPAR gamma agonists is maintained in cells expressing a PPAR gamma dominant-negative mutant: evidence for selectivity in the downstream responses to PPAR gamma activation. Mol Endocrinol. 2001; 15:1729–1738. [PubMed: 11579205]

21. Overkleeft HS, Renkema GH, Neele J, Vianello P, Hung IO, Strijland A, van der Burg AM, Koomen GJ, Pandit UK, Aerts JM. Generation of specific deoxynojirimycin-type inhibitors of the non-lysosomal glucosylceramidase. J Biol Chem. 1998; 273:26522–26527. [PubMed: 9756888]
22. Folch J, Lees M, Sloane Stanley GH. A simple method for the isolation and purification of total lipids from animal tissues. J Biol Chem. 1957; 226:497–509. [PubMed: 13428781]
23. Taketomi T, Hara A, Uemura K, Sugiyama E. Rapid method of preparation of lysoglycosphingolipids and their confirmation by delayed extraction matrix-assisted laser desorption ionization time-of-flight mass spectrometry. J Biochem (Tokyo). 1996; 120:573–579. [PubMed: 8902623]
24. Neville DC, Coquard V, Priestman DA, te Vruchte DJ, Sillence DJ, Dwek RA, Platt FM, Butters TD. Analysis of fluorescently labeled glycosphingo-lipid-derived oligosaccharides following ceramide glycanase digestion and anthranilic acid labeling. Anal Biochem. 2004; 331:275–282. [PubMed: 15265733]
25. Van Weely S, Van Leeuwen MB, Jansen ID, De Bruijn MA, Brouwer-Kelder EM, Schram AW, Sa Miranda MC, Barranger JA, Petersen EM, Goldblatt J, Stotz H, Schwarzmann G, Sandhoff K, Svennerholm L, Erikson A, Tager JM, Aerts JM. Clinical phenotype of Gaucher disease in relation to properties of mutant glucocerebrosidase in cultured fibroblasts. Biochim Biophys Acta. 1991; 1096:301–311. [PubMed: 1829642]
26. Andersson U, Butters TD, Dwek RA, Platt FM. N-butyldeoxygalactonojirimycin: a more selective inhibitor of glycosphingolipid biosynthesis than N-butyldeoxynojirimycin, in vitro and in vivo. Biochem Pharmacol. 2000; 59:821–829. [PubMed: 10718340]
27. Andersson U, Reinkensmeier G, Butters TD, Dwek RA, Platt FM. Inhibition of glycogen breakdown by iminosugars in vitro and in vivo. Biochem Pharmacol. 2004; 67:697–705. [PubMed: 14757169]
28. Ebina Y, Edery M, Ellis L, Standring D, Beaudoin J, Roth R, Rutter WJ. Expression of a functional human insulin receptor from a cloned cDNA in Chinese hamster ovary cells. Proc Natl Acad Sci U S A. 1985; 82:8014–8018. [PubMed: 3906655]
29. van Dijk TH, Boer TS, Havinga R, Stellaard F, Kuipers F, Reijngoud DJ. Quantification of hepatic carbohydrate metabolism in conscious mice using serial blood and urine spots. Anal Biochem. 2003; 322:1–13. [PubMed: 14705774]
30. Grefhorst A, van Dijk TH, Hammer A, van der Sluijs FH, Havinga R, Havekes LM, Romijn JA, Groot PH, Reijngoud DJ, Kuipers F. Differential effects of pharmacological liver X receptor activation on hepatic and peripheral insulin sensitivity in lean and ob/ob mice. Am J Physiol Endocrinol Metab. 2005; 289:E829–E838. [PubMed: 15941783]
31. Cox T, Lachmann R, Hollak C, Aerts J, van Weely S, Hrebicek M, Platt F, Butters T, Dwek R, Moyses C, Gow I, Elstein D, Zimran A. Novel oral treatment of Gaucher's disease with N-butyldeoxynojirimycin (OGT918) to decrease substrate biosynthesis. Lancet. 2000; 355:1481–1485. [PubMed: 10801168]
32. Yildiz Y, Matern H, Thompson B, Allegood JC, Warren RL, Ramirez DM, Hammer RE, Hamra FK, Matern S, Russell DW. Mutation of beta-glucosidase 2 causes glycolipid storage disease and impaired male fertility. J Clin Invest. 2006; 116:2985–2994. [PubMed: 17080196]
33. Boot RG, Verhoek M, Donker-Koopman W, Strijland A, van Marle J, Overkleeft HS, Wennekes T, Aerts JM. Identification of the non-lysosomal glucosylceramidase as beta-glucosidase 2. J Biol Chem. 2006; 282:1305–1312. [PubMed: 17105727]
34. Scott LJ, Spencer CM. Miglitol: a review of its therapeutic potential in type 2 diabetes mellitus. Drugs. 2000; 59:521–549. [PubMed: 10776834]
35. Fleet GW, Fellows LE, Winchester B. Plagiarizing plants: amino sugars as a class of glycosidase inhibitors. Ciba Found Symp. 1990; 154:112–122. [PubMed: 2150798]
36. Nojima H, Kimura I, Chen FJ, Sugihara Y, Haruno M, Kato A, Asano N. Antihyperglycemic effects of N-containing sugars from Xanthocercis zambesiaca, Morus bombycis, Aglaonema treubii, and Castanospermum australe in streptozotocin-diabetic mice. J Nat Prod. 1998; 61:397–400. [PubMed: 9544568]

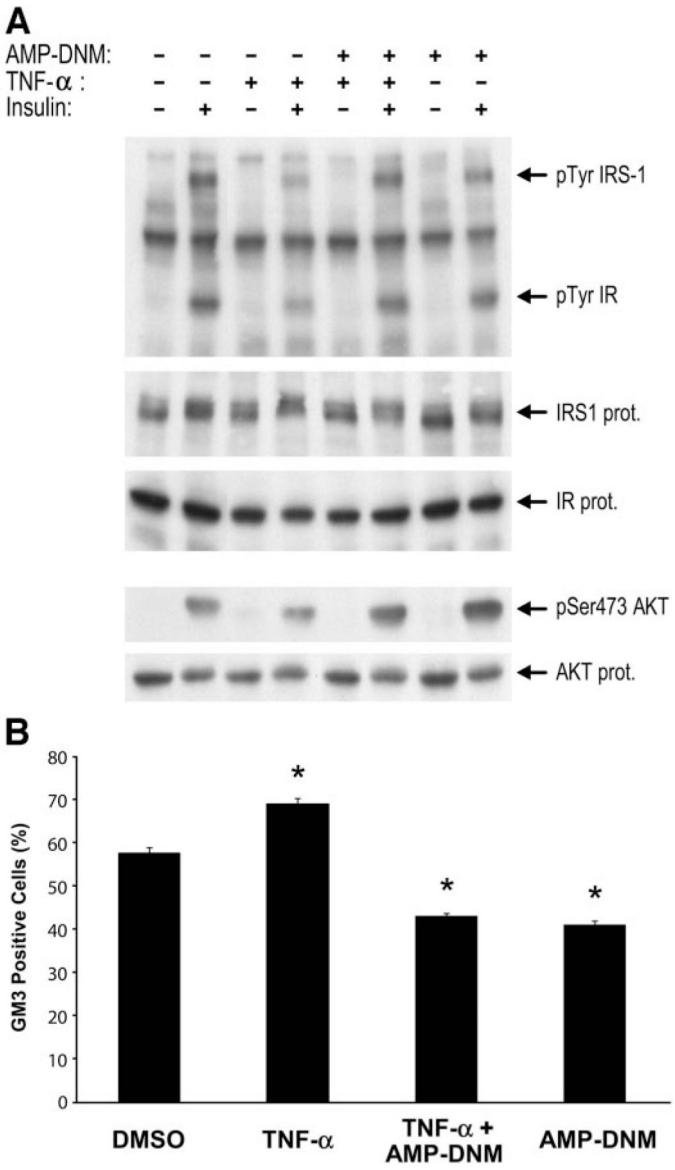

FIG. 1.

AMP-DNM reverses TNF-α-induced insulin resistance and surface expression of GM3 in 3T3-L1 adipocytes. Serum-starved 3T3-L1 adipocytes were treated with either vehicle/control, AMP-DNM (10 μmol/l), and/or TNF-α (0.6 nmol/l) for 24 h before stimulation with or without insulin (100 nmol/l for 5 min). *A*: Immunoblots of whole-cell lysates were performed in parallel as described in RESEARCH DESIGN AND METHODS. Representative blots are shown from one of three independent experiments. *B*: Cell surface expression of GM3 was determined on basal adipocytes (not stimulated with insulin) by fluorescence-activated cell sorter analysis. Values represent means ± SE of viable cells that stained positive for GM3. **P* < 0.05; observed in four independent experiments.

Europe PMC Funders Author Manuscripts

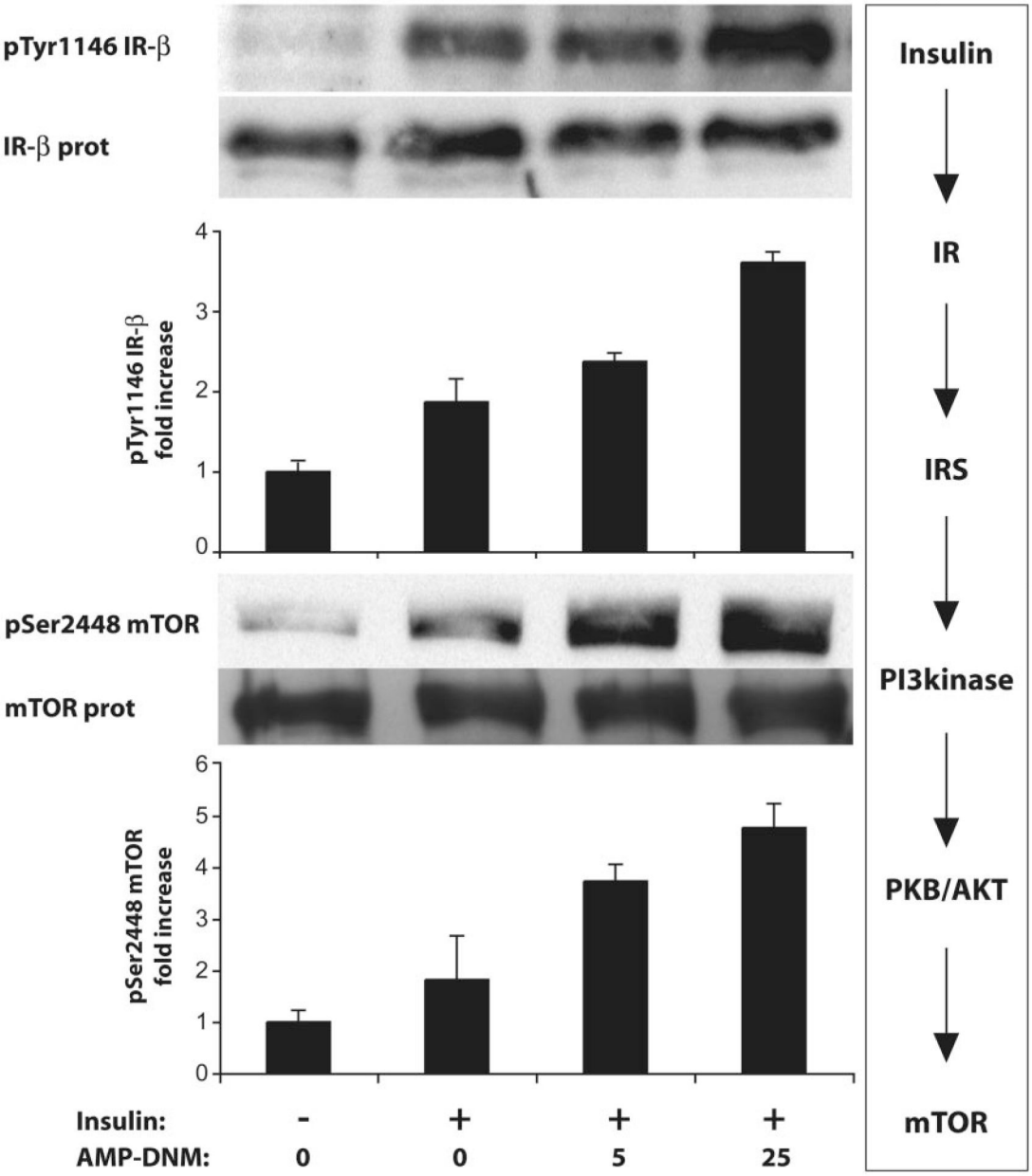

FIG. 2.

Improved insulin signaling in the liver of *ob/ob* mice treated with AMP-DNM. Animals were fed for 2 weeks with 0, 5, or 25 mg AMP-DNM/kg. To animals starved overnight, insulin (0.75 units/kg) was administered via the vena porta. Livers were collected after 5 min. Insulin receptor protein, and its autophosphorylation, and mTOR protein, and its serine phosphorylation, were visualized and quantified.

Europe PMC Funders Author Manuscripts

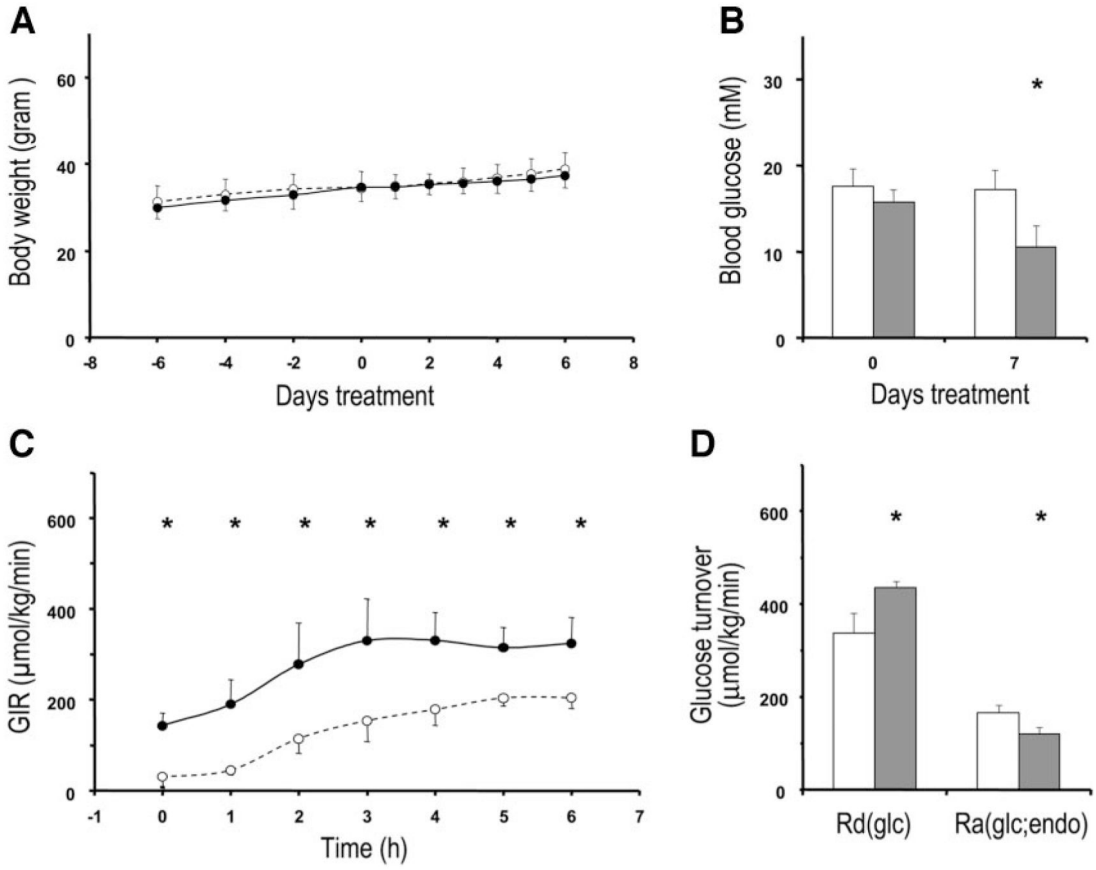

FIG. 3.

Beneficial effects of iminosugar feeding on glucose metabolism in *ob/ob* mice. *ob*/*ob* mice were fed either a control diet (○ and □) or with diet providing a dose of 25 mg AMP-DNM · kg body $wt^{-1} \cdot day^{-1}$ (● and ■). Body weight (*A*) and blood glucose levels (*B*) were determined at indicated time points. During the clamp, glucose infusion rate (GIR) was monitored (*C*), the rate of glucose disposal [Rd(glc)], and the rate of endogenous hepatic glucose production [Ra(glc;endo)] were calculated (*D*). Data presented are means ± SD. Significant differences between both groups (*) are indicated. Statistical significances of differences were determined using Student's *t* test, except in calculations over time where ANOVA with repeated measurements was used. $P < 0.05$ was considered statistically significant.

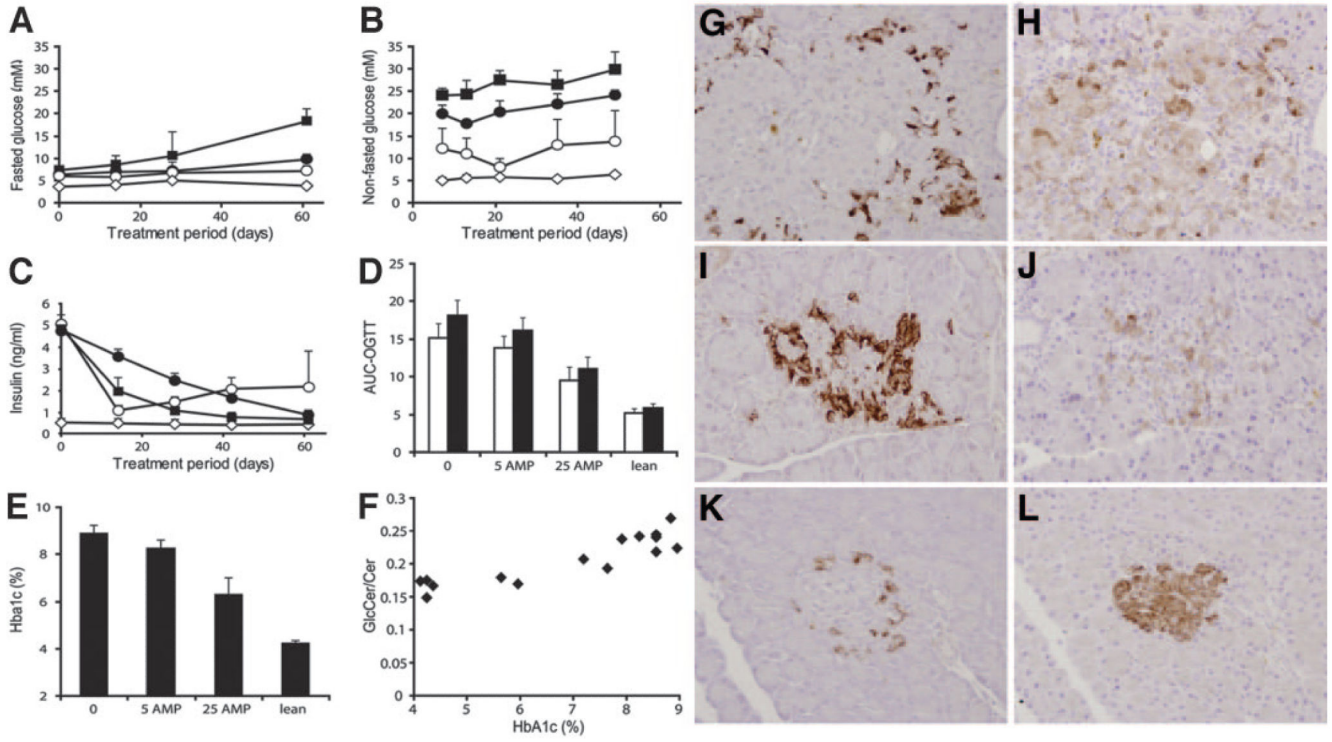

FIG. 4.

Beneficial effects of iminosugar feeding in ZDF rats. ZDF rats (10 weeks old) were treated for 10 weeks with 0, 5, or 25 mg AMP-DNM · kg^{-1} · day^{-1} (n = 4 for each group). As a control, lean littermates were analyzed. Presented are means ± SD. *A*: Fasted blood glucose during treatment period. *B*: Nonfasted blood glucose during treatment period. *C*: Plasma insulin levels during treatment period. *D*: Oral glucose tolerance at week 2 (□) and week 9 (■) of treatment. *E*: A1C after 10 weeks of treatment. *F*: Relation of level of A1C (%) with hepatic glucosylceramide–to–ceramide ratio (GlcCer/Cer). Values are means ± SD. *G*: Pancreas glucagon immunostaining placebo-treated ZDF rats. *H*: Pancreas insulin immunostaining placebo-treated ZDF rats. *I*: Pancreas glucagon immunostaining 25 mg AMP-DNM–treated ZDF rats. *J*: Pancreas insulin immunostaining 25 mg AMP-DNM–treated ZDF rats. *K*: Pancreas glucagon immunostaining lean littermate. *L*: Pancreas insulin immunostaining lean littermate. ■, 0 mg AMP-DNM · kg^{-1} · day^{-1}; ●, 5 mg AMP-DNM · kg^{-1} · day^{-1}; ○, 25 mg AMP-DNM · kg^{-1} · day^{-1}; ◇, lean rats.

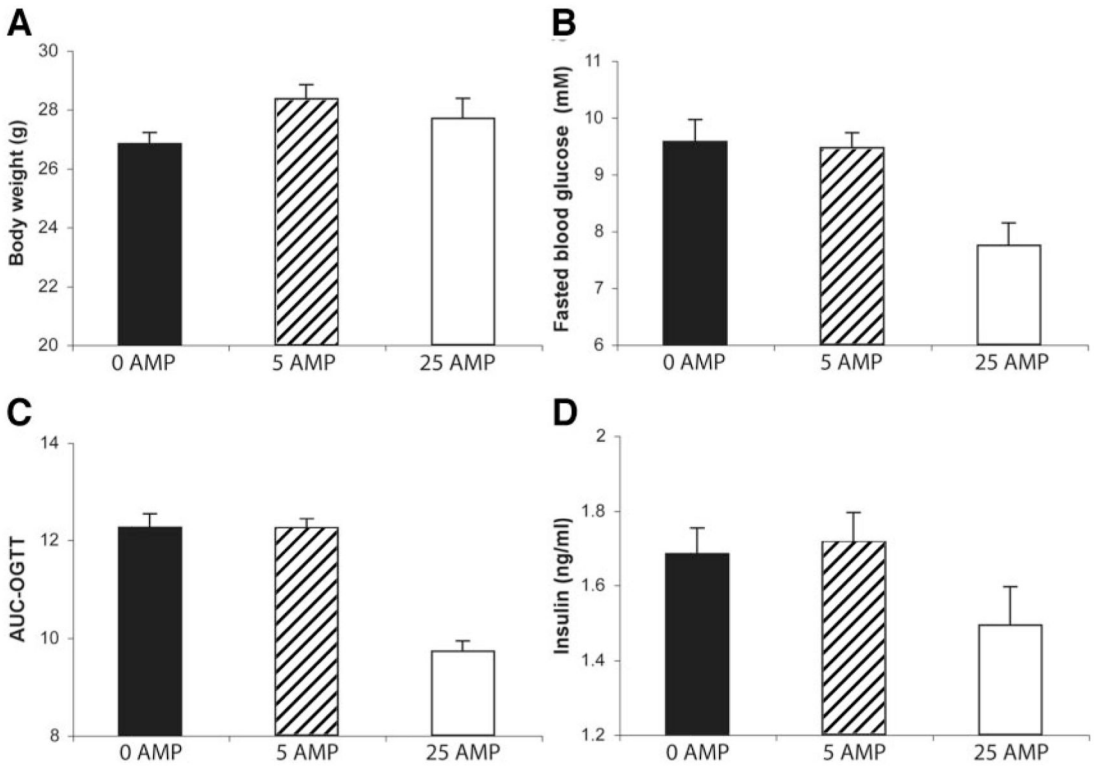

FIG. 5.

Beneficial effects of AMP-DNM on glucose homeostasis in diet-induced glucose-intolerant mice. Glucose-intolerant C57Bl/6J mice were obtained after a high-fat diet for 4 weeks. For 2 weeks, two groups of eight animals were administered, by daily oral gavage, 0, 5, and 25 mg AMP-DNM $\cdot$ kg^{-1} $\cdot$ day^{-1}. Values represent means ± SD. *A*: Body weight. *B*: Fasted blood glucose. *C*: Oral glucose tolerance (expressed as AUC). *D*: Plasma insulin.

Europe PMC Funders Author Manuscripts

TABLE 1

Effect of AMP-DNM on ceramide and glycosphingolipids in 3T3-L1 adipocytes

Sphingolipid (pmol/well)	Ceramide	GM3	GM2
Without insulin			
No addition	957 ± 71	2,192 ± 144	335 ± 21
With TNF	1,328 ± 95	3,265 ± 225	442 ± 20
With AMP-DNM	970 ± 57	1,063 ± 65	170 ± 12
With TNF + AMP-DNM	1,241 ± 88	2,205 ± 138	267 ± 18
With insulin			
No addition	955 ± 56	2,451 ± 184	382 ± 26
With TNF	1,492 ± 92	4,288 ± 321	619 ± 36
With AMP-DNM	1,096 ± 56	1,074 ± 87	175 ± 10
With TNF + AMP-DNM	1,241 ± 99	1,988 ± 169	267 ± 97

Data are means ± SE. Serum-starved 3T3-L1 adipocytes were treated with either vehicle/control, AMP-DNM (10 μmol/l), and/or TNF-α (0.6 nmol/l) for 24 h prior to stimulation with or without insulin (100 nmol/l for 5 min). Sphingolipid content was determined by HPLC-based procedures as described in RESEARCH DESIGN AND METHODS. Values represent means of four wells. Similar results were obtained in two independent experiments.

Europe PMC Funders Author Manuscripts

TABLE 2

Effect of AMP-DNM on ceramide and glucosylceramide content of liver and muscle of *ob/ob* and normal C57Bl/6J mice

	GlcCer (nmol/mg protein)	Cer (nmol/mg protein)
Liver		
Normal: 0 mg AMP-DNM	2.12 ± 0.15	9.44 ± 0.82
Normal: 25 mg AMP-DNM	1.24 ± 0.09*	10.31 ± 0.96
ob/ob: 0 mg AMP-DNM	3.81 ± 0.24	102.6 ± 12.3
ob/ob: 25 mg AMP-DNM	2.24 ± 0.14*	95.9 ± 11.6
Muscle		
Normal: 0 mg AMP-DNM	1.48 ± 0.31	1.42 ± 0.60
Normal: 25 mg AMP-DNM	0.89 ± 0.22*	1.47 ± 0.22
ob/ob: 0 mg AMP-DNM	2.49 ± 0.41	1.21 ± 0.31
ob/ob: 25 mg AMP-DNM	1.41 ± 0.16*	1.29 ± 0.24

Data are means ± SD. Animals were fed for 2 weeks with 0 or 25 mg AMP-DNM/kg. Liver and muscle tissue were collected and analyzed on ceramide and glucosylceramide content by HPLC-based procedures described in RESEARCH DESIGN AND METHODS. Values represent the mean of four animals.

Cer, ceramide; GlcCer, glucosylceramide-to-ceramide ratio.

* $P < 0.05$ by Student's *t* test (0 vs. 25 mg treatment group).

Europe PMC Funders Author Manuscripts

TABLE 3

Ceramide and glycosphingolipid levels in liver of normal and ZDF rats treated with AMP-DNM

Liver sphingolipid (nmol/g wet wt)	0 mg AMP-DNM · kg^{-1} · day^{-1}	5 mg AMP-DNM · kg^{-1} · day^{-1}	25 mg AMP-DNM · kg^{-1} · day^{-1}	Normal littermate
Ceramide	461 ± 29	416 ± 24	451 ± 37	475 ± 25
Glucosylceramide	56.7 ± 9.2	53.4 ± 5.7	47.4 ± 5.2	46.1 ± 5.0
Gangliosides				
GM3	22.5 ± 3.2	21.3 ± 2.9	17.3 ± 2.7	20.0 ± 2.2
GM2	6.2 ± 1.0	5.9 ± 0.9	4.8 ± 0.8	5.0 ± 0.4
GM1	11.6 ± 2.9	11.4 ± 2.2	5.6 ± 1.1	9.1 ± 1.5
GDA1	15.7 ± 1.5	15.5 ± 1.7	7.9 ± 0.9	16.4 ± 1.2

Data are means ± SD. Animals were fed for 10 weeks with 0, 5, or 25 mg AMP-DNM/kg. Liver was collected and analyzed on ceramide, glucosylceramide, and ganglioside content.